Angular distribution of γ rays from the p-wave resonance of ^{118}Sn

J. Koga,[1,*] S. Takada ,[1] S. Endo ,[2,3] H. Fujioka ,[4] K. Hirota ,[3,†] K. Ishizaki,[3] A. Kimura,[2] M. Kitaguchi ,[3] Y. Niinomi,[3] T. Okudaira ,[3] K. Sakai,[2] T. Shima,[5] H. M. Shimizu ,[3] Y. Tani,[4] T. Yamamoto,[3] H. Yoshikawa ,[5] and T. Yoshioka [1,‡]

^{1}*Kyushu University, 744 Motooka, Nishi-ku, Fukuoka 819-0395, Japan*
^{2}*Japan Atomic Energy Agency, 2-1 Shirane, Tokai 319-1195, Japan*
^{3}*Nagoya University, Furocho, Chikusa, Nagoya 464-8062, Japan*
^{4}*Tokyo Institute of Techonology, Meguro, Tokyo 152-8511, Japan*
^{5}*Osaka University, Ibaraki, Osaka 567-0047, Japan*

The neutron energy-dependent angular distribution of γ rays from the ^{117}Sn(n, γ) reaction was measured with germanium detectors and a pulsed neutron beam. The angular distribution was clearly observed in γ-ray emissions with an energy of 9327 keV which corresponds to the transition from a neutron resonance of ^{117}Sn $+n$ to the ground state of ^{118}Sn. The angular distribution causes an angular-dependent asymmetric resonance shape. An asymmetry A_{LH} was defined as $(N_{\mathrm{L}} - N_{\mathrm{H}})/(N_{\mathrm{L}} + N_{\mathrm{H}})$, where N_{L} and N_{H} are integrated values for lower- and higher-energy regions of a neutron resonance, respectively. We found that the A_{LH} has the angular dependence of $(A \cos \theta_\gamma + B)$, where θ_γ is the γ-ray emission angle with respect to the incident neutron momentum, with $A = 0.394 \pm 0.073$ and $B = 0.118 \pm 0.029$ in the 1.33 eV p-wave resonance.

I. INTRODUCTION

Neutron resonances in medium-mass nuclei are expected as one of the sensitive probes for symmetry-breaking physics. A large parity violation (P violation) has been observed as the helicity dependence of the neutron-capture cross section at p-wave resonances in various nuclei [1]. These large P-violating effects are explained as a result of the interference between the amplitudes of p-wave resonances and the neighboring s-wave resonances (sp-mixing model). In addition, it is predicted that the violation of time-reversal symmetry (T violation) can be also enhanced by the same mechanism based on the sp-mixing model [2], which enables a sensitive search for T violation using a neutron-induced compound state. The understanding of the enhancement mechanism of P/T violation based on the sp-mixing model will therefore bring a knowledge of P/T violation in elementary processes.

Flambaum and Sushkov reported that the sp mixing causes a neutron energy-dependent angular distribution of γ rays in the vicinity of a p-wave resonance with respect to the incident neutron momentum [3]. The first measurement of angular distribution was conducted for the (n, γ) reactions of ^{117}Sn $+n$ at the IBR-30 reactor, located at the Laboratory of Neutron Physics, JINR in 1985 [4]. The angular distribution was observed using two NaI(Tl) spectrometers at $90 + \theta$ and $90 - \theta$ degrees with respect to the neutron beam

axis. Because an energy difference between the ground and the first excited states of ^{117}Sn $+n$ is more than 1000 keV, even the γ-ray energy resolution of NaI spectrometers can separate their states. In addition, a left-right asymmetry in the emission of γ rays was obtained by the measurement with polarized neutron beam [4].

Recently, thanks to a high γ-ray energy resolution of germanium detectors at the accurate neutron-nucleus reaction and measurement (ANNRI) in the Japan Proton Accelerator Research Complex (J-PARC), we can measure the angular distribution for each transition with a large signal to background ratio [5–7]. Moreover, the neutron-energy resolution is better than that of the reactor due to the benefit of the pulsed neutron source. In this paper, we report the angular distribution of γ rays from the 1.33 eV p-wave resonance of ^{117}Sn $+n$ to the ground state of ^{118}Sn measured at more angles than in the previous study by using a germanium detector assembly and the intense neutron beam at J-PARC. The more detailed information of the angular distribution will advance the understanding of the sp-mixing model.

II. EXPERIMENT

The measurement was performed using ANNRI installed at the beamline 04 (BL04) of the Material and Life Science Experiment Facility (MLF) in J-PARC. A pulsed neutron beam was produced by the nuclear spallation reactions and was slowed down by a liquid hydrogen moderator. The neutron beam was transported to the target position located at 21.5 m from the moderator surface, and a germanium detector assembly which consists of 22 germanium detectors was used

---

*Corresponding author: junkoga@kyudai.jp

†Present address: High Energy Accelerator Research Organization, 1-1 Oho, Tsukuba, Ibaraki 305-0801, Japan.

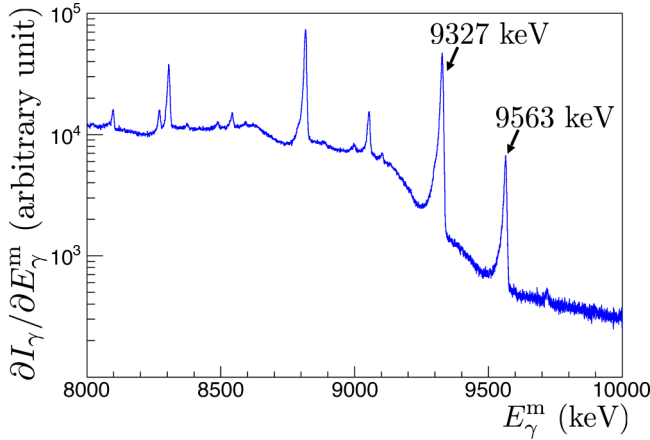‡Corresponding author: yoshioka@phys.kyushu-u.ac.jp

FIG. 1. Histogram of $\partial I_\gamma / \partial E_\gamma^{\mathrm{m}}$ in the range of 8–10 MeV.

FIG. 2. Histogram of $\partial I_\gamma / \partial E_n^{\mathrm{m}}$ in the range of 0–10 eV. In this histogram, γ rays whose energies were below about 200 keV were eliminated. The peak of 1.33 eV is a *p*-wave resonance of ^{118}Sn.

to detect γ rays emitted from the target. A more detailed explanation for the experimental setup is described in Ref. [5].

The target was a tin plate with dimensions of $40 \times 40 \times 4$ mm^3 and natural isotopic abundance, hence 7.68% of ^{117}Sn. The chemical purity was 99.9%. The total measurement time was about 65 h with a proton beam power of 150 kW. The deposited γ-ray energy calibration was performed by full-absorption peaks of γ rays emitted from the ^{27}Al(n, γ) reactions.

Figure 1 shows the spectrum of the deposited γ-ray energy (E_γ^{m}) in all detectors defined as $\partial I_\gamma / \partial E_\gamma^{\mathrm{m}}$. Here, I_γ denotes the number of detected γ rays in the experiment. The γ transition from the compound state of ^{118}Sn to the ground state with the energy of 9327 keV can be seen clearly. It is known that the compound state in the *p*-wave resonance decays to the ground state of ^{118}Sn directly. Therefore, we focused our analysis on the peak with 9327 keV. The γ-ray peak of 9563 keV stemmed from the ^{115}Sn(n, γ) reactions.

The incident neutron energy E_n^{m} was calculated using the kinetic energy formula of classical mechanics substituting the time (t^{m}) from the proton-beam injection into the MLF moderator to the arrival of neutrons at the tin target. Figure 2 shows a histogram defined as $\partial I_\gamma / \partial E_n^{\mathrm{m}}$. In this histogram, γ rays whose energies were below about 200 keV were eliminated by energy thresholds of a data acquisition system. The peak of 1.33 eV is a *p*-wave resonance of ^{118}Sn of interest to us. One can see an *s*-wave resonance of ^{116}In at 1.46 eV and a *p*-wave resonance of ^{120}Sn at 6.22 eV. Because the cross section of the 1.46 eV *s*-wave resonance is about 10^4 times larger than that of the 1.33 eV *p*-wave resonance, their count rates become comparable even if the target is contaminated by 0.01% of ^{115}In. The pulse heights information was lost about 2% of total γ-ray counts in the 1.33 eV *p*-wave resonance region, which was corrected in the following analysis. The ratio of events that two signals are regarded as a single event was estimated as 0.3% of total γ-ray counts in the 1.33 eV *p*-wave resonance region, which is negligibly small compared with the statistical error of the γ-ray peak counts focused in this study.

The cross section for the (n, γ) reaction is expressed by the Breit-Wigner function described by resonance parameters: resonance energy E_r, total angular momentum J_r, orbital
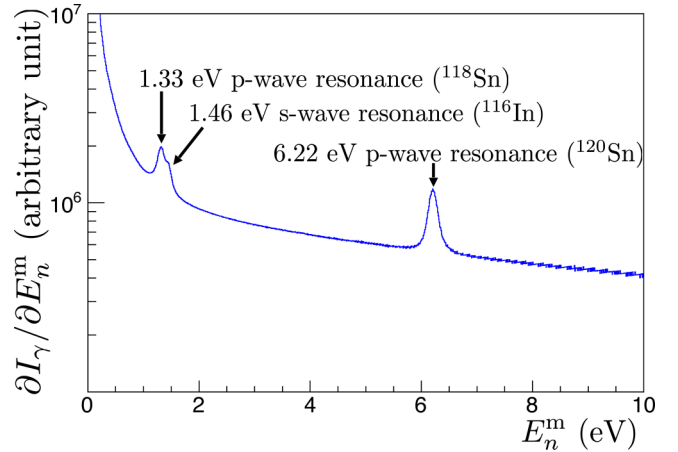
angular momentum l_r, γ width Γ_r^γ, statistical factor g_r, and neutron width Γ_r^n. Here, the subscript r means an *s*-wave or a *p*-wave resonance. The resonance parameters of the *p*-wave resonance were measured using a ^{117}Sn-enriched tin target. The measurement time was about 3 h with the proton beam power of 525 kW. The resonance parameters were determined by fitting the *p*-wave resonance gated with $E_\gamma^{\mathrm{m}} \geqslant 2$ MeV using the Breit-Wigner function convoluted with the Doppler broadening effect and the time structure of the pulsed neutron beam [8]. In this work, the resonance energy and the γ width of the *p*-wave resonance were obtained as $E_p = 1.331 \pm 0.002$ eV and $\Gamma_p^\gamma = 133 \pm 5$ meV. In the fitting, other resonance parameters were fixed at published values: $J_p = 1$, $l_p = 1$, and $g_p \Gamma_p^n = 1.38 \times 10^{-4}$ meV [9].

III. ANALYSIS

The histogram gated with the 9327 keV full-absorption peak includes background events from other sources than the resonance of interest in ^{118}Sn. Here, the gate range was defined as the full width at quarter maximum (FWQM). There are two main kinds of background events. One is the Compton scattering of γ rays with 9563 keV. The other is caused by pileup events due to simultaneous detection of multi γ rays. These background events must be subtracted. First, the number of such events in the signal region was estimated using a GEANT4 simulation [10]. In this simulation, a response function of the detector assembly can be calculated, and a spectrum of monochromatic γ-ray energy can be reproduced by emitting γ rays from the target position. Figure 3 shows the histograms of $\partial I_\gamma / \partial E_\gamma^{\mathrm{m}}$ for each background event. Histograms gated with the background regions (9563 keV peak and energies higher than 9600 keV) were scaled so that number of events in the signal region matched that of simulated ones in the γ-ray energy spectrum. After that, they were subtracted from the histogram gated with the signal regions.

In the epithermal energy region, the neutron-beam intensity at J-PARC increases for lower neutron energies as a result of moderation. The histogram defined by $\partial I_\gamma / \partial E_n^{\mathrm{m}}$ must be
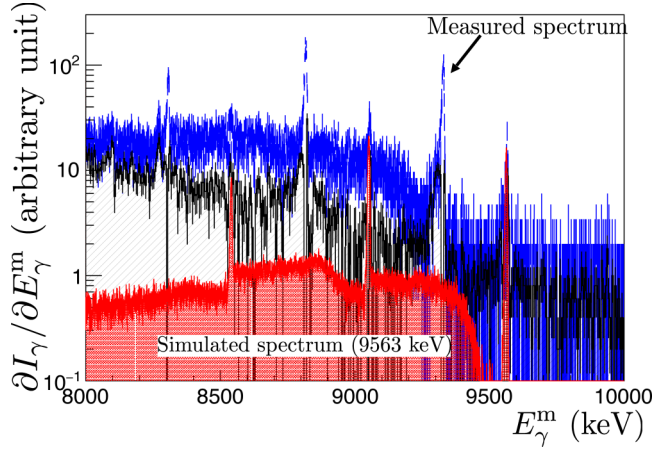
FIG. 3. Histograms of $\partial I_\gamma / \partial E_\gamma^{\mathrm{m}}$ for each background event. Blue-open histogram is the measured spectrum. Red-hatched one is a simulated spectrum for monochromatic energy of 9563 keV. This was scaled so that the intensity of the full-absorption peak matched that of the measured one. Black-striped histogram is the spectrum of pileup events which were obtained by subtracting the red-hatched spectrum and a simulated spectrum of monochromatic energy of 9327 keV.

normalized to obtain the neutron-energy dependence of the 1.33 eV p-wave resonance shape. The energy dependence of incident neutron beam was obtained by measuring the 477.6 keV γ rays emitted by the ^{10}B$(n, \alpha\gamma)$^{7}Li reactions with a boron target. The ^{10}B$(n, \alpha\gamma)$^{7}Li reaction is suitable to obtain the energy dependence of the neutron beam because there are no resonances in the epithermal region [$\mathcal{O}(1$ eV$)$]. The beam intensity $\psi(E_n^{\mathrm{m}})$, as a function of neutron energy E_n, can be represented as

$$\psi\left(E_n^{\mathrm{m}}\right) = \frac{I\left(E_n^{\mathrm{m}}\right)}{\sigma(E_n)\epsilon T}, \tag{1}$$

where $\sigma(E_n)$ is the cross section of the ^{10}B$(n, \alpha\gamma)$^{7}Li reaction, which is 3837 ± 9 b for 2200 m/s neutrons [11] and is assumed to be dependent on neutron velocity v based on the $1/v$ law. The $I(E_n^{\mathrm{m}})$ is the number of the 477.6 keV γ rays detected during the measurement time T, and ϵ is the detection efficiency of each germanium detector at 477.6 keV.

The effective photopeak efficiency of each germanium detector, including the solid angle coverage of each crystal, is different from each other. The effective photopeak efficiency was determined relatively based on the assumption
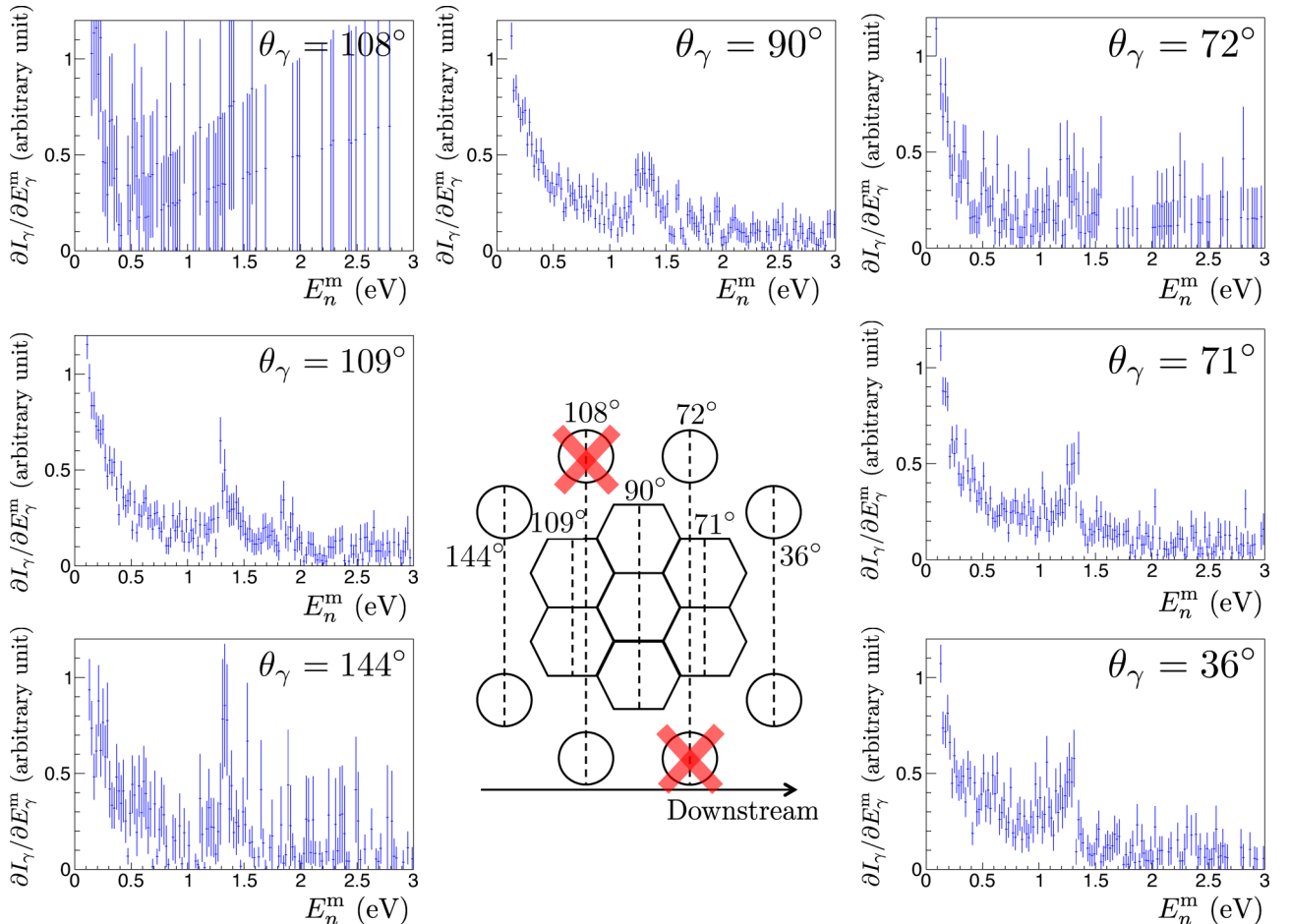

FIG. 4. Histograms of $\partial I_\gamma / \partial E_n^{\mathrm{m}}$ around the 1.33 eV p-wave resonance in ^{118}Sn for various angles accessible at ANNRI. The central figure shows the placement and shape of each germanium crystal. The detectors marked by red crosses were not used in this measurement.
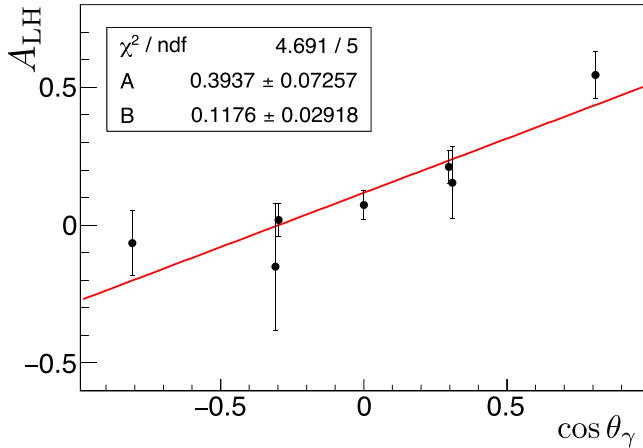
FIG. 5. Fitting result for $A_{\mathrm{LH}}(\theta_\gamma)$ using Eq. (3). The angular-dependent parameter A were obtained to be a significant value.

that prompt γ rays from ^{14}N(n, γ) reactions of a melamine target were emitted isotropically. Figure 4 shows histograms as a function of E_n^{m} around the 1.33 eV p-wave resonance for various angles. The E_n^{m} dependence of the angular distribution can be observed as an asymmetric resonance shape in the histograms of $\partial I_\gamma / \partial E_n^{\mathrm{m}}$.

IV. DISCUSSION

To evaluate the E_n^{m} dependence of the angular distribution of γ rays, an asymmetry $A_{\mathrm{LH}}(\theta_\gamma)$ was used as in the analysis for lanthanum [5]. The asymmetry $A_{\mathrm{LH}}(\theta_\gamma)$ is defined as

$$A_{\mathrm{LH}}(\theta_\gamma) = \frac{N_{\mathrm{L}}(\theta_\gamma) - N_{\mathrm{H}}(\theta_\gamma)}{N_{\mathrm{L}}(\theta_\gamma) + N_{\mathrm{H}}(\theta_\gamma)}, \tag{2}$$

where θ_γ is the γ-ray emission angle with respect to the neutron momentum, and this asymmetry can be parametrized as

$$A_{\mathrm{LH}}(\theta_\gamma) = A \cos \theta_\gamma + B. \tag{3}$$

Here, the subscripts L and H represent "low energy region" and "high energy region", respectively. The regions for integration were defined using the p-wave resonance energy E_p and the total resonance width Γ_p as follows: $E_p - 2\Gamma_p <$

$E_n < E_p$ for $N_{\mathrm{L}}(\theta)$ and $E_p < E_n < E_p + 2\Gamma_p$ for $N_{\mathrm{H}}(\theta)$. The total resonance width is defined as $\Gamma_p = \Gamma_p^\gamma + \Gamma_p^n$. Here, the resonance parameters, E_p, Γ_p^γ, and Γ_p^n, were the values described in Sec. II.

The asymmetry $A_{\mathrm{LH}}(\theta_\gamma)$ can be fitted using Eq. (3), and the fitting result is shown in Fig. 5. The parameters of the $A_{\mathrm{LH}}(\theta_\gamma)$ were obtained as

$$A = 0.394 \pm 0.073 \text{ and } B = 0.118 \pm 0.029. \tag{4}$$

Significant E_n^{m} dependence of the angular distribution was observed in the vicinity of the p-wave resonance.

V. CONCLUSION

The experiment was conducted for measuring the E_n^{m} dependence of angular distribution of γ rays in the transition from the p-wave resonance of ^{117}Sn $+n$ to the ground state of ^{118}Sn at BL04 ANNRI in J-PARC MLF. The E_n^{m} dependence of angular distribution of γ rays was significantly observed, and the angular-dependent asymmetric resonance shape was evaluated using the asymmetry value $A_{\mathrm{LH}}(\theta_\gamma)$. The angular dependence of the asymmetry $A_{\mathrm{LH}}(\theta_\gamma)$ was obtained as $A_{\mathrm{LH}}(\theta_\gamma) = A \cos \theta_\gamma + B$ with $A = 0.394 \pm 0.073$ and $B = 0.118 \pm 0.029$. This result and future measurements of angular distributions of γ rays with polarized neutron beam will allow for cross checking with the previous result, which will advance the understanding of sp-mixing model of compound states.

[1] G. E. Mitchell, J. D. Bowman, S. I. Pentillä, and E. I. Sharapov, Phys. Rep. **354**, 157 (2001).

[2] V. P. Gudkov, Phys. Rep. **212**, 77 (1992).

[3] V. V. Flambaum and O. P. Sushkov, Nucl. Phys. A **435**, 352 (1985).

[4] V. P. Alfimenkov, S. B. Borzakov, Yu. D. Mareev, L. B. Pikelner, A. S. Khrykin, and E. I. Sharapov, Rapid Communication No. 10-85, JINR, Dubna (1985), p. 19.

[5] T. Okudaira, S. Takada, K. Hirota, A. Kimura, M. Kitaguchi, J. Koga, K. Nagamoto, T. Nakao, A. Okada, K. Sakai, H. M. Shimizu, T. Yamamoto, and T. Yoshioka, Phys. Rev. C **97**, 034622 (2018).

[6] T. Yamamoto, T. Okudaira, S. Endo, H. Fujioka, K. Hirota, T. Ino, K. Ishizaki, A. Kimura, M. Kitaguchi, J. Koga, S. Makise, Y. Niinomi, T. Oku, K. Sakai, T. Shima, H. M. Shimizu, S. Takada, Y. Tani, H. Yoshikawa, and T. Yoshioka, Phys. Rev. C **101**, 064624 (2020).

[7] T. Okudaira, S. Endo, H. Fujioka, K. Hirota, K. Ishizaki, A. Kimura, M. Kitaguchi, J. Koga, Y. Niinomi, K. Sakai, T. Shima, H. M. Shimizu, S. Takada, Y. Tani, T. Yamamoto, H. Yoshikawa, and T. Yoshioka, Phys. Rev. C **104**, 014601 (2021).

[8] K. Kino, M. Furusaka, F. Hirata, T. Kamiyama, Y. Kiyanagi, K. Furutaka, S. Goto, K. Y. Hara, H. Harada, K. Hirose, T. Kai, A. Kimura, T. Kin, F. Kitatani, M. Koizumi, F. Maezawa, S. Meigo, S. Nakamura, M. Ooi, M. Ohta *et al.*, Nucl. Instrum. Methods Phys. Res. A **736**, 66 (2014).

[9] D. A. Smith, J. D. Bowman, B. E. Crawford, C. A. Grossmann, T. Haseyama, M. B. Johnson, A. Masaike, Y. Matsuda, G. E. Mitchell, V. A. Nazarenko, S. I. Penttila, N. R. Roberson, S. J. Seestrom, E. I. Sharapov, L. M. Smotritsky, S. L. Stephenson, and V. Yuan, Phys. Rev. C **59**, 2836 (1999).

[10] S. Takada, T. Okudaira, F. Goto, K. Hirota, A. Kimura, M. Kitaguchi, J. Koga, T. Nakao, K. Sakai, H. M. Shimizu, T. Yamamoto, and T. Yoshioka, J. Instrum. **13**, P02018 (2018).

[11] S. F. Mughabghab, *Atlas of Neutron Resonances*, 5th ed. (Elsevier, Amsterdam, 2006).